J Mater Sci: Mater Med (2008) 19:2889–2901
DOI 10.1007/s10856-008-3437-y

# On the possibility of silicon nitride as a ceramic for structural orthopaedic implants. Part II: chemical stability and wear resistance in body environment

**Mauro Mazzocchi · Davide Gardini · Pier Luigi Traverso · Maria Giulia Faga · Alida Bellosi**

Received: 26 April 2007 / Accepted: 10 August 2007 / Published online: 15 April 2008
© Springer Science+Business Media, LLC 2008

**Abstract** In Part I, the processing, microstructure and mechanical properties of three silicon nitride-based ceramics were examined and their non-toxicity was demonstrated. In this Part II, some features critical to biomedical applications were investigated: (i) the wetting behaviour against aqueous media, including physiological solutions; (ii) the chemical stability in water and in physiological solutions; and (iii) the wear resistance, measured under experimental procedures that simulate the conditions typical of the hip joint prosthesis. The results confirmed that silicon nitride may serve as a biomaterial for bone substitution in load bearing prosthesis.

## 1 Introduction

Silicon nitride-based ceramics present a combination of mechanical, tribological, thermal and chemical properties that makes them suitable for high performance components in severe environments in several industrial applications. In the introduction of Part I [1], a detailed state of the art is presented, concerning the potentialities and the open problems for the use of silicon nitride in orthopaedic and dental applications [2–11] in the human body. Among the parts for biomedical applications that could be made of silicon nitride, the most important are the followings [12–16]: total joint replacements, minifixation systems, drug delivery supports, micro-mechanical devices, intervertebral spacers, implants in traumatology. However, there are still some controversy in the literature about the biocompatibility [2–7], as indicated in Part I [1].

The absence of toxic behaviour and the biocompatibility were ascertained during toxicity tests and in-vivo tests [1, 7, 17–20]. Silicon nitride does not induce inflammation while promoting the proliferation of osteoblast cells [20]. It was reported that cell growth on polished silicon nitride surface, viability and morphology are comparable to parameters of titanium [21]. However there are studies [15, 22] according to which the non-oxide ceramics do not offer sufficient potential for implants in joint arthroplasty.

Generally silicon nitride-based ceramics can be regarded as ceramic-glass composites, because of the addition of sintering aids that are necessary for the densification to occur, but originate partially amorphous grain boundary phases [23, 24]. The glassy phases exhibit bioactivities different from pure silicon nitride.

For total artificial joints, ceramic–ceramic joints have become more and more popular as long-term replacement. The majority of the ceramic–ceramic prostheses currently used consist of alumina–alumina parts. Alumina–alumina coupling has many advantages but also the drawback that friction and wear are not the lowest in the ceramic–ceramic combinations [3]. In bearing surfaces the wear is still one of the key factors under investigation [12–15] and it is necessary to look for improved ceramic–ceramic wear couples for innovative total joint replacements.

M. Mazzocchi (✉) · D. Gardini · A. Bellosi
Institute for Sciences and Technology for Ceramics, National Research Council, Via Granarolo, n.64, Faenza, Ravenna 48018, Italy
e-mail: mauro.mazzocchi@istec.cnr.it

P. L. Traverso
Harine Sciences Institute-Unit in Genova, National Research Council, Via De Marini, n.6, Genova 16149, Italy

M. G. Faga
Institute for Sciences and Technology for Ceramics-Unit in Torino, National Research Council, Strada Delle Cacce, n.7, Torino 10135, Italy

In the high precision ceramic-on-ceramic total joint prosthesis with very low wear, significant fluid film form for small radial clearance during walking. The lubricant effectiveness depends on the wetting properties, i.e. on the surface adhesion of the polar liquids which are the natural lubricant of the joints [13, 14, 25–29].

The wetting properties of the surfaces are important for the broad issue of biocompatibility. They influence solid–liquid interaction, lubrication, tissue adhesion. All these features are important parameters for biological effects at cell level, like affinity, adhesiveness, protein adsorption.

Furthermore, the surface wettability has a significant influence on the friction and wear behaviour of a tribological system, as in the direct contact between ceramic bearing surfaces. It gives an indication of its biotolerance, which is directly related to the materials combination and lubricants. In a first approximation, the more wettable the material, the better the human body tolerates it [25–28].

The present paper examines some key properties of three silicon nitride-based ceramics: wettability and interfacial interaction with different liquid lubricants, surface modification due to the contact with liquid media and tribological behaviour. The processing procedures, microstructure, mechanical properties and cytotoxicity of the three materials, with properly designed sintering aids and secondary phase, were investigated in Part I [1].

## 2 Materials and methods

### 2.1 Materials

The dense silicon nitride-based materials were fabricated by hot pressing, starting from the following powder mixtures: A: 90.0 vol.% $Si_3N_4$ + 10.0 vol.% bioactive glass; B: 91.3 vol.% $Si_3N_4$ + 8.7 vol.% MgO; C: 65.0 vol.% (93 wt.% $Si_3N_4$ + 2 wt.% $Al_2O_3$ + 5 wt.% $Y_2O_3$) + 35.0 vol.% TiN.

The composition (in wt.%) of the used bioactive glass is: $SiO_2$ 43.94, $P_2O_5$ 10.27, CaO 31.93, $Na_2O$ 4.55, $K_2O$ 0.19, MgO 2.79, $CaF_2$ 4.94, $Ta_2O_5$ 0.99, $La_2O_3$ 0.50; its in vitro and in vivo performances were previously extensively studied [30, 31].

Details on the processing procedures and on the microstructure are described in Part I [1].

The liquid media used for the tests objectives of this study are the followings:

- ultrapure deionised water (electrical resistivity: 18 MΩcm), coded as W;
- isotonic saline physiological solution (NaCl 0.9 wt.%) (Eurospital SpA, Italy), as PHS1;
- Hank's Balanced Salt Solution (HBSS modified, Sigma–Aldrich Co., USA), as PHS2;
- Dilute bovine serum (BS), consisting of 75% of water and 25 vol.% of calf BS (Sigma–Aldrich Co., USA), with addiction of $Na_3N$ as antibacterial agent in the concentration of 1 g $l^{-1}$, coded BS.

### 2.2 Materials characterization

#### *2.2.1 Surface roughness*

The surface roughness is a key factor in determining many phenomena: the wetting behaviour against liquids, the reactivity at the solid/liquid interfaces, the wear behaviour under tribological conditions, the biological response like adhesion of protein, the cell attachments and so on.

Considering the role and the effects of the surface morphology on the behaviour and properties related to the interaction between two parts in contact and on the determination of hydrophobicity, roughness measurements were performed upon the polished surface of the samples used for wetting tests by sessile drop technique and for tribological tests. The surfaces were prepared using the same procedures, i.e. polishing with diamond pastes up to 1 μm.

A Taylor Hobson Ltd. Talysurf PGI Plus prophilometer (Gaussian filter, band width: 300) was used to measure the roughness. The characteristic parameters were calculated: Ra, the arithmetic mean deviation of the assessed profile, i.e. the average deviation of the trace from the computed centre line, and Rt, the total height of the profile, i.e. the sum of the maximum profile peak and the maximum profile valley depth. The values of the surface roughness, considering a sampling length of 0.8 mm, were reported in Table 1.

#### *2.2.2 Wettability*

In order to determine the surface and interfacial interaction that take place in solid bioceramics in contact with liquid media, the measure of the contact angle was carried on, selecting three different liquids: deionized water (W), Hank's solution (PHS2) and BS. The sessile drop technique was applied using an optical tensiometer equipped with a CCD video camera with a rate of image acquisition of 25 frames per second and a resolution of 752 × 582 pixels (OCA 15+, DataPhysics Instr. GmbH, Germany). Drops of 1 μl were deposited on the surfaces, at room temperature, through flat needles with outer diameter of 0.51 mm. The outline of the drops was recorded and analyzed with the Laplace-Young method from the instant of their deposition and till 5 s, when the spreading motion is over and the contact angle values tend to a plateau. Longer times were avoided either because is important the early surface interaction between the biological fluids and the solid surface or in order to prevent changes over time of the

**Table 1** Surface roughness (Rt and Ra) of the three silicon nitride-based ceramics surfaces and contact angles in function of the lubricant (W, water; PHS2, Hank's solution; BS, bovine serum)

| Solid surface | Rt (μm) | Ra (μm) | Liquid drop | Contact angle (°) |
|---|---|---|---|---|
| $Si_3N_4$–bioactive glass | 0.55 ± 0.10 | 0.06 ± 0.01 | W | 46.5 |
| | | | PHS2 | 42.6 |
| | | | BS | 50.1 |
| $Si_3N_4$–MgO | 0.96 ± 0.20 | 0.07 ± 0.01 | W | 58.7 |
| | | | PHS2 | 45.4 |
| | | | BS | 40.3 |
| $Si_3N_4$–TiN | 0.41 ± 0.10 | 0.04 ± 0.01 | W | 61.4 |
| | | | PHS2 | 65.4 |
| | | | BS | 59.2 |
| $Al_2O_3$ | 1.2 ± 0.30 | 0.06 ± 0.01 | W | 71.9 |
| | | | PHS2 | 42.2 |
| | | | BS | 58.7 |
| $ZrO_2$ (Y-PSZ) | 0.40 ± 0.30 | 0.03 ± 0.01 | W | 81.2 |
| | | | PHS2 | 62.6 |
| | | | BS | 63.6 |
| $Al_2O_3$–$ZrO_2$ (80/20) | 1.0 ± 0.10 | 0.04 ± 0.01 | W | 88.4 |
| | | | PSH2 | 69.8 |
| | | | BS | 54.1 |

contact angle deriving from secondary effects like solid/liquid reactions, protein adsorption and liquid evaporation. To avoid the needles climbing of the BS liquid, their surfaces were pre-treated with a perfluorated substance. The mean values of contact angle at plateau, averaged over different drops, for the three silicon nitride-based materials were reported in Table 1 along with the results on other solid bioceramics—high purity alumina (Almatis CT3000 SG), Y-PSZ zirconia (Tosoh TZ-3YB) and alumina/zirconia composite (a mixture between CT3000 SG and TZ-3YB, with a wt% ratio 80:20)—as comparison.

### 2.2.3 *Chemical stability and corrosion resistance in aqueous environments*

The surface modifications, indicating the stability in aqueous environments, for the three silicon nitride-based ceramics were studied at 37°C using as liquid media water (W) and the isotonic saline physiological solution (PHS1). The duration of the tests was 45 days.

Ceramic samples were machined in small prism shapes and, subsequently, one of their surfaces was polished with diamond paste (0.25 μm finer grain size). In next steps of 30 min each one, the samples were cleaned by ultrasonic bath in trichloroethylene, acetone and ethanol; a final ultrasonic treatment in ultrapure deionised water for one hour was carried out. Then the samples were dried at 80°C for 12 h, weighed and put into about 50 ml of W and PHS1 contained in glass vials. The six glass vials were previously cleaned with a 0.1 M $HNO_3$ solution and carefully rinsed with ultrapure deionised water. Finally, each vial, containing the liquid and the ceramic sample, was sealed by Parafilm pellicle, put in stand in a thermostatic bath at 37°C and stirred every day.

After 45 days the samples were extracted from the liquids, rinsed with ultrapure deionized water, dried at 100°C for 15 min and, at last, weighed again. The weight changes are shown in Table 2.

The polished surfaces, after the 45 days contact with the liquids, were analysed by X-ray Photoelectronic Spectrophotometer (XPS). The peculiar feature of this analytical technique is to provide information on the chemical bonds and on the element quantity relating to the first 4–5 atomic layers (about 20 Å in deep). A VG ESCALAB 210 XPS spectrometer (Thermo VG Scientific Ltd, UK) with a spherical sector analyser and unmonocromatized MgKα (E = 1,253.6 eV) was used as excitation source. Spectra were collected in a vacuum higher than $10^{-8}$ mbar with a detection angle normal to the surface. Binding energies were determined with reference to Au $4f_{7/2}$, Ag $3d_{5/2}$ and Cu $2p_{3/2}$; C 1 s binding energy (285.1 ± 0.1 eV) of hydrocarbon contamination was used to compensate for charging effects. Qualitative analyses were carried out by the correlation with the binding energies of the different peaks with corresponding elements. Quantitative analyses were made by software using the Scofield sensitivity factors and expressed in atomic percentage. In order to obtain different peaks corresponding to the different compounds of the same element, curve fitting was carried out by the reduced $\chi^2$ method.

The microstructure of the sample surfaces after the chemical stability test was also observed by scanning electron microscope (SEM) and energy dispersion spectrophotometer (EDS) analyses to investigate morphological and chemical modifications.

### 2.2.4 *Wear resistance*

Friction and wear tests were done employing a CSM High Temperature Tribometer (CSM Instruments SA, Switzerland). In this apparatus a rotating disk is in contact with a static element, on which the load is applied. The static element used during the sliding tests is an alumina ball,

**Table 2** Weight changes of the three silicon nitride-based ceramics after 45 days at 37°C in contact with water (W) and saline physiological solution (PHS1)

| Sample | Δ wt. (W) (mg) | Δ wt. (PHS1) (mg) |
|---|---|---|
| $Si_3N_4$–bioactive glass | −0.35 | −0.52 |
| $Si_3N_4$–MgO | +0.10 | −0.72 |
| $Si_3N_4$–TiN | +0.16 | +0.46 |

since the contact condition in a hip joint may be approximated by a sphere on a plane contact.

The size of the ball was 6 mm in diameter, while the silicon nitride disc-shaped samples were 30 mm in diameter and 5 mm in thickness.

A load of 7–10 N was applied during the ball on disc test; linear velocities of 10, 25 and 32 cm $s^{-1}$, respectively, were used for the sample revolutions. 790, 2,200 and 12,000 m (corresponding to 25,000, 50,000 and 200,000 revolutions) were run. Dilute BS was used as lubricant medium during the tests carried out at 37°C.

Wear quantification was obtained measuring the wear track by a Taylor Hobson Ltd. Talysurf PGI Plus prophilometer, while the ball wear was measured with a digital camera microscope interfaced with a PC. The worn areas on the samples were observed by an SEM equipped with EDS.

## 3 Results and discussion

### 3.1 Wettability

The wettability of water (W), Hank's solution (PHS2) and BS on the surfaces of the three silicon nitride-based ceramics was evaluated measuring the contact angle by the sessile drop method. The main purpose is to design the proper material composition and surface conditions to enhance the lubrication. Basically, the smaller the contact angles of the drop on the ceramic surface, the better the lubrication.

Table 1 and Fig. 1 summarize the results of the contact angle measurements achieved on the three silicon nitride-based ceramics with respect the three liquids, comparing them to three oxide ceramics usually employed as bioceramics: alumina, zirconia and alumina/zirconia composite (the last one being constituted by an alumina matrix containing 20 wt.% of zirconia). Table 1 shows also the values of the roughness of the surfaces where the measure of contact angle was performed. The Ra values of the three silicon nitride-based ceramics range from 0.04 to 0.07 μm and can be considered ultra-smooth. The lowest roughness was measured on zirconia (0.03 μm), which undergo an easier material removal under polishing, because its hardness is lower (Hv ~12 GPa) than alumina (Hv ~18 GPa) and silicon nitride (Hv ~15–19 GPa) ones.

The shapes of the water drops and of the drops of PHS2 solution on the surfaces of the three silicon nitride-based ceramics, compared to the shapes of the same liquids on alumina put in evidence the higher affinity of the liquids towards silicon nitride rather than towards alumina (Fig. 2a–d).

The contact angles of water on the three silicon nitride-based ceramics are significantly lower than the values measured on the oxides and confirm a more hydrophilic

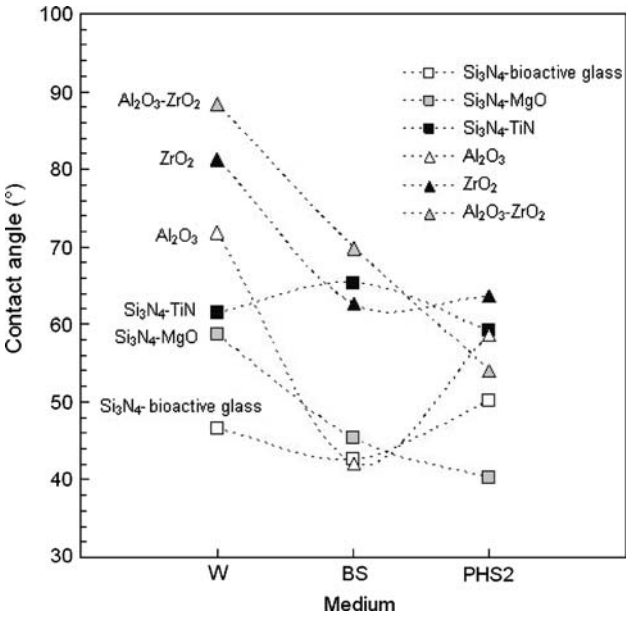


**Fig. 1** Contact angles between W, PHS2, BS media, for the three silicon nitride-based ceramics and for the three oxides alumina, zirconia and alumina–zirconia composite

character of silicon nitride than alumina and zirconia, as also previously reported [26, 27, 29, 32]. The relatively high contact angles of pure oxides and their composites have been explained [29] on the basis of the energies of interaction at the solid/liquid interface, that have been attributed to dispersion-London forces interactions. Instead, the $SiO_2$-containing oxides present a better affinity towards water because polar forces act at the interface, in addition to the dispersion ones, and the contact angle decreases in function of the amount of glassy phase [29]. Actually, in the present study the measured contact angles relative to silicon nitride-based materials range from 61.4° to 46.5°. The differences can be related to the presence and amount of glassy silicate phase: the lowest contact angle (46.5°) concerns the silicon nitride ceramic with 10 vol.% of bioactive glass, while the sample produced with the addition of 8.7 vol.% of MgO (contact angle 58.7°) contains about 5 vol.% of a crystalline magnesium silicate phase (detected by XRD analysis). The $Si_3N_4$–TiN composite (contact angle 61.4°) has the lowest amount of grain boundary glassy phase, estimated in the range 3–4 vol.%. The relationship between the amount of amorphous silicates and the affinity towards water is supported by the data shown in literature [27], where a contact angle of 26.6° was measured on a $Si_3N_4$-30 vol.% bioactive glass composite. The same work reports an increasing contact angle using as wetting agents either a simulated body fluid and a BS [27]. Instead, the results achieved in the present study do not evidence a unique behaviour: in the $Si_3N_4$–bioactive glass the contact angle of the Hank's PHS2 slightly decreases,

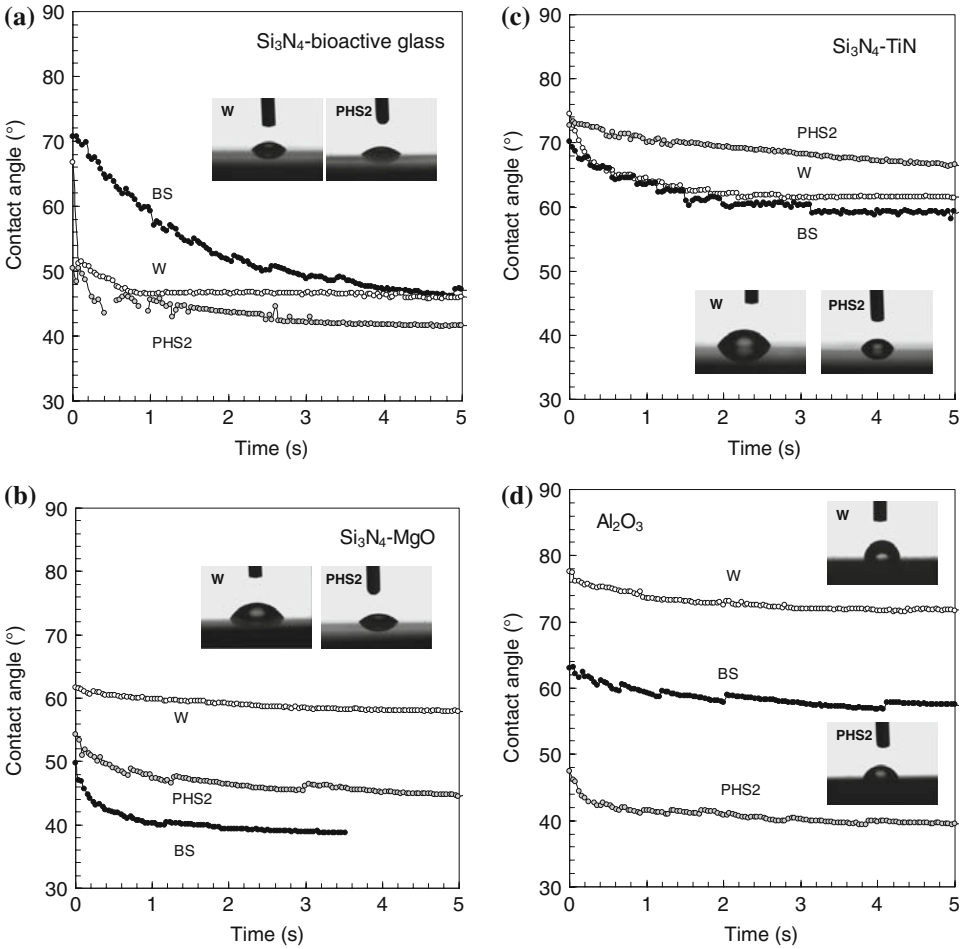


**Fig. 2** **(a–d)** Evolution with time of contact angles of W, PHS2 and BS after their deposition on the polished surfaces of $Si_3N_4$–bioactive glass (**a**), $Si_3N_4$–MgO (**b**), $Si_3N_4$–TiN (**c**), alumina samples (**d**)

while that of the BS increase until about 50°. The contact angle of PHS2 on $Si_3N_4$–MgO is similar to that on $Si_3N_4$–bioactive glass, but the contact angle of BS is the lowest measured. The $Si_3N_4$–TiN composite evidences a small variation in the wetting behaviour, independently on the liquids. The three oxides (alumina, zirconia and alumina–zirconia) reveal a strong increase of wettability moving on from water to the Hank's PHS2. When in contact with this latter liquid, alumina shows the lowest contact angle, similar to the two monolithic silicon nitride ceramics ($Si_3N_4$–bioactive glass and $Si_3N_4$–MgO). Instead, the wettability of the three oxides against BS is not very different, although higher than the one exhibited by the two monolithic silicon nitrides.

Chemical and morphological nature of biomaterials surface determine to a large extent either the interactions between bioceramics and host tissue and physiological fluids or the phenomena which occur at the contact under load with another determining surface wear and degradation. Therefore, it is mandatory to correlate the above reported results about wettability with the surface chemical and physical properties. The roughness data do not show significant differences (Table 1), therefore the different values in the contact angles should be attribute to the surface charges and related physicochemical phenomena rather than to morphological differences of the exposed surface. A quantitative indicator of hydrophilicity is given by the polarity; among the three materials the most hydrophilic is $Si_3N_4$–bioactive glass. There is an increase in hydrophilicity with higher relative portions of glassy phase in the silicon nitride. However, the three silicon nitride-based ceramics are more hydrophilic than the tested oxides: alumina, zirconia and alumina–zirconia composite. The different behaviours can be related to the polar surface energy component (compared to the dispersive one) governing the surface tension [27], associated with the volume of $SiO_2$-containing phases [29] in the silicon nitride-based ceramics. The same argument can be proposed to explain the different wettability against water of the three silicon nitride materials.

The nature of the intermolecular forces established between the solid surface and the aqueous biological liquids depend on the surface chemical composition. In the case of $Si_3N_4$ powders, it was demonstrated that the surface reactivity of silicon nitride induces the formation of a few nanometres thick layer [33, 34], composed by $Si_2N_2O$ [35] and containing mainly silanol (Si–OH) and secondary

amine groups ($Si_2$–NH). As a result, the surface charge in aqueous media is negative above the isoelectric point [35]. If the phenomena observed on the particles surface can be considered valid also for the surface of bulk silicon nitride in water, then the $Si_3N_4$ surface charge is the result of the preferential equilibria between the surface functional groups and Si–O unsaturated bonds, governed by the presence of $OH^-$.

The relationships between the contact angles of the other liquids (physiological solution and BS) are quite complex. Dealing with BS, the decrease of the contact angle has been previously attributed [27] to the transport of albumin (a pre-requisite for cell attachment) to the surface of the drop with a consequent decrease of the surface tension. The absorption of albumin on different ceramics [34] is related to the surface charges; $Si_3N_4$ is characterized by a negative $\zeta$-potential and high adsorption of albumin, although other chemical and physical factors influence the phenomena. Some explanations about the relationships between the adsorption behaviour of albumin at the surface of silicon nitride are given in previous works [27, 36].

Molecular rearrangement on surface, soluble phases, surface groups are among the factors determining the contact angles between the ceramics and complex liquids like physiological solutions and BS.

### 3.2 Chemical stability and corrosion resistance in aqueous environments

The analyses performed on the surfaces of samples soaked for 45 days at 37°C in W or PHS1 consisted in the measure of the weight changes of the samples (Table 2), of the elemental concentration and of chemical alteration detected by XPS (Table 3, Fig. 3) and in the evaluation of the microstructure of the surfaces (Figs. 4a, b, 5, 6a, b, for the samples $Si_3N_4$–bioactive glass, $Si_3N_4$–MgO and $Si_3N_4$–TiN, respectively).

**Table 3** XPS elemental concentration (at wt.%) for the different samples surfaces before and after the 45-days soaking tests at 37°C in water (W) and saline physiological solution (PHS1)

| Sample | Environment | Si | N | O | Mg | Ti |
|---|---|---|---|---|---|---|
| $Si_3N_4$–bioactive glass | Virgin surface | 40.1 | 40.2 | 19.7 | – | – |
| | W | 37.4 | 38.8 | 23.8 | – | – |
| | PHS1 | 38.2 | 41.3 | 20.5 | – | – |
| $Si_3N_4$–MgO | Virgin surface | 38.2 | 41.4 | 18.1 | 2.3 | – |
| | W | 38.3 | 47.8 | 12.8 | 1.1 | – |
| | PHS1 | 37.9 | 45.0 | 16.3 | 0.8 | – |
| $Si_3N_4$–TiN | Virgin surface | 34.5 | 39.4 | 24.3 | – | 1.8 |
| | W | 35.1 | 43.1 | 20.3 | – | 1.5 |
| | PHS1 | 31.0 | 33.4 | 34.2 | – | 1.4 |

At a first glance the data collected in Table 2 point out a very limited interaction between the ceramic and the liquids, however, in some cases there is a weight loss ($Si_3N_4$–bioactive glass in W and PHS1 and $Si_3N_4$–MgO in PHS1), in other cases a weight gain ($Si_3N_4$–MgO in PHS1 and $Si_3N_4$–TiN in both the environments). In the following these data are discussed with those deriving from the XPS analyses and from the morphological modification observed on the sample surfaces by SEM and EDS.

$Si_3N_4$–bioactive glass shows a slight weight loss which indicate that there was been a corrosion, although very limited, when exposed under the two testing conditions. The XPS analyses evidence that when immersed in water the surfaces enrich of different oxygen-containing phases, associated to a clear increase of the full width at half maximum of the intensity profile (FWHM factor) in the XPS spectra (Fig. 3), that passes from 2.3 eV in the spectrum of the starting sample (Fig. 3a) to 3.2 eV in the spectra of the two exposed surfaces (Fig. 3b). At the same time, the slight decrease of Si and N indicate a low dissolution of silicon nitride (Table 3). The chemical interaction between water and the ceramic surface can be explained by two concurrent phenomena: the dissolution of silicon nitride and the consequent formation of silica. Figure 4a shows that nano-sized spherical particles, probably silica, nucleate on the surface and contain oxygen in amount higher than in the matrix material as revealed by EDS analyses. The effect on grain boundary phases, if any, cannot be revealed with the adopted analytical technique. No evident modification was revealed on the same surface after the test under physiological solution (Fig. 4b). Probably the same phenomena above described occur, but in still less extent. It is possible that a very scarce leaching of grain boundary phase occur in some areas where these phases concentrate. However, the surface modification and reactivity are very low.

After the exposure in both the aqueous environments $Si_3N_4$–MgO reveals a surface modification that involve mainly the leaching of the grain boundary phase, as pointed out by XPS data (Table 3) and from SEM analyses (Fig. 5). On the treated surface, oxygen and magnesium, forming the grain boundary phases, are lower than in the starting surface. It is not possible to assess the formation of surface silica, even though the oxidation reaction of silicon nitride takes place, the newly formed phases are at nano-size level.

The composite $Si_3N_4$–TiN evidences the most relevant modifications among the three tested materials, particularly after the test in physiological solution (Figs. 6a, b). The main features observed are: (i) the grain boundary phase, which is concentrated at triple points or in selected pockets, undergoes to a partial dissolution; (ii) new oxide phases form by reaction either of $Si_3N_4$ to silica, or of TiN to titanium oxide, as assessed by the elemental analysis of the

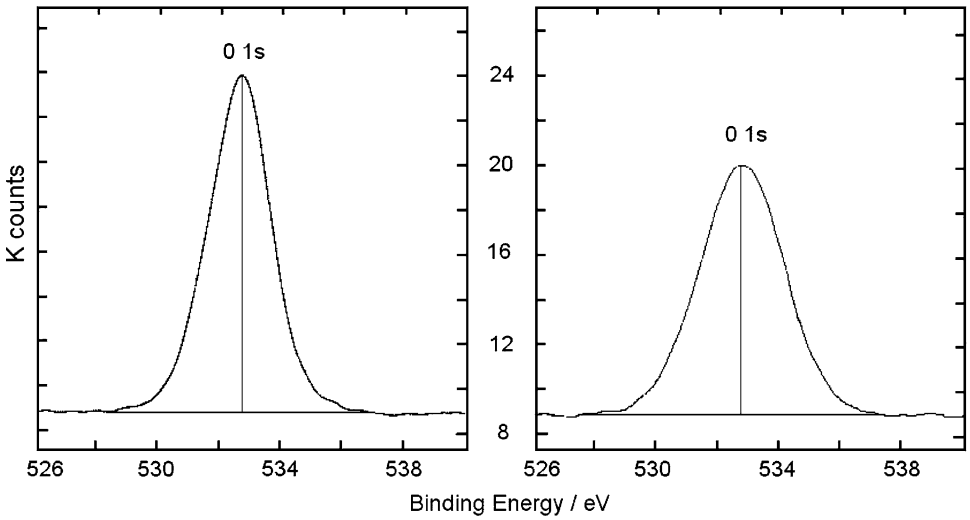


**Fig. 3** XPS analysis patterns taken on $Si_3N_4$–bioactive glass polished surfaces samples before (left) and after soaking in $H_2O$ prolonged for 45 days (right). The comparison between the two patterns evidences the increase of full width at half maximum (FWHM) factor as a result of an increase in oxygen containing phases after the permanence in the liquid medium

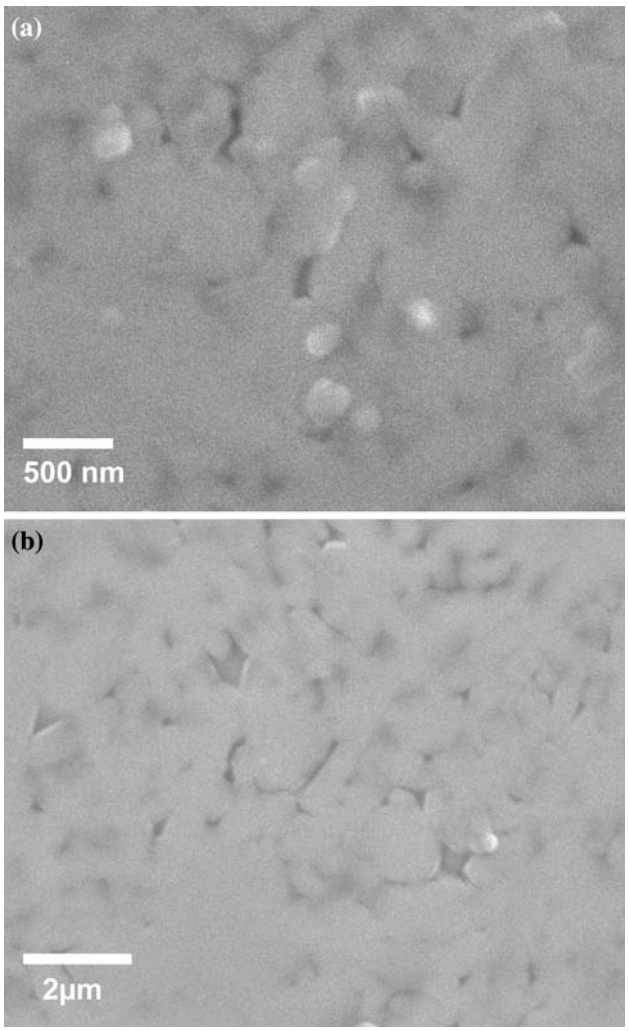


**Fig. 4** (**a**, **b**) $Si_3N_4$–bioactive glass polished surface microstructure after 45 days soaking in $H_2O$ (**a**) and after 45 days soaking in PHS1(**b**)

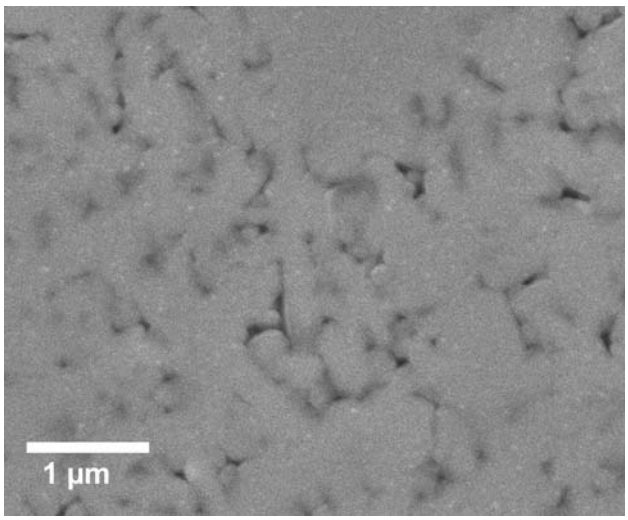


**Fig. 5** $Si_3N_4$–MgO polished surface sample after 45 days soaking in PHS1

surface and by the surface morphology of the samples; (iii) the surface oxidation effects account for the measured weight gain after the exposure test (Table 2).

### 3.3 Wear resistance

Ball-on-disk test is commonly used to obtain information about the friction coefficient and the wear behaviour of lot of materials, as bulk or coatings, which can find application in several fields. For joint prostheses in biomedical applications, evaluating the mutual wear resistance of a couple of bearing surfaces is a key issue. Even though the tests can not perfectly simulate the movement in the real system, sliding contact tests allow: (i) to forecast which couple of materials can behave as the highest wear resistant; (ii) to

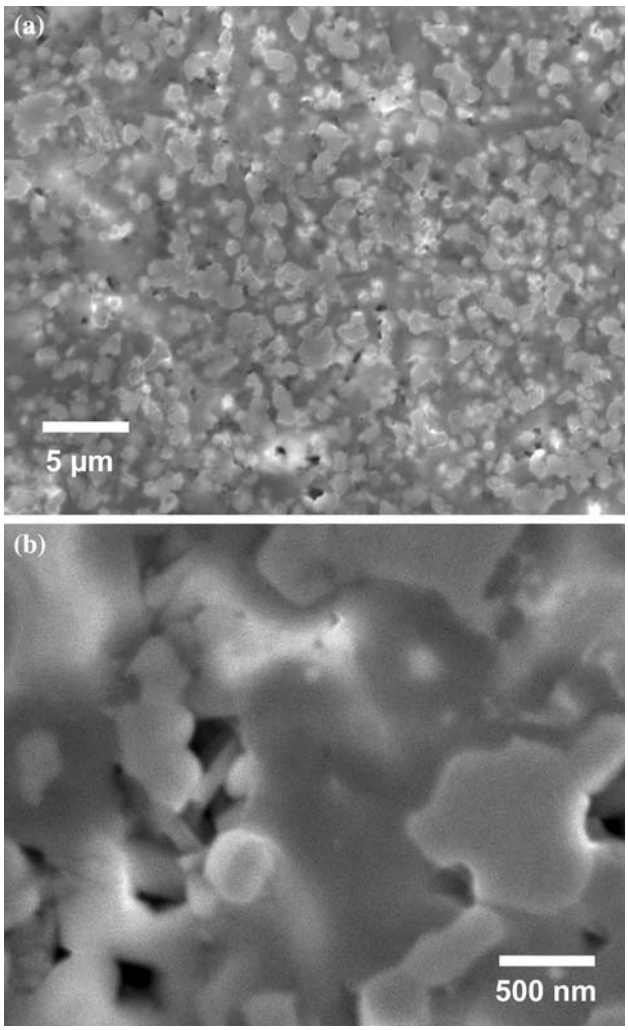


**Fig. 6** (**a**, **b**) $Si_3N_4$–TiN polished surface sample after 45 days soaking in $H_2O$ (**a**) and after 45 days soaking in PHS1 (**b**)

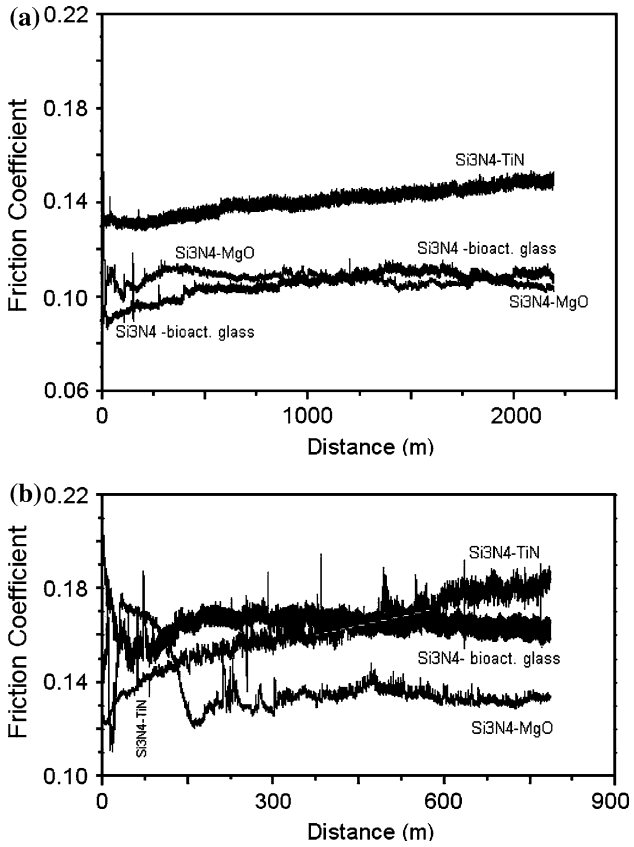


**Fig. 7** (**a**, **b**) Evolution of friction coefficients versus covered distance on disc-shaped samples (37°C; dilute bovine serum). Experimental conditions (instr. precision ± 0.02) of 25 cm $s^{-1}$, 10 N, 2,200 revolutions (**a**); 10 cm $s^{-1}$, 7 N, 790 revolutions (**b**)

estimate the friction coefficient under different conditions. Alumina is one of the most used ceramic material as component in hip prosthesis, as the bearing surface of metal alloys devices, often coupled to ultra high molecular weight polyethylene (UHWMPE) or alumina itself [15]. Among them, the best wear couple was found to be alumina–alumina, leading to a wear rate of less than 1 μm per year. Due to this reason, such high wear resistance oxide was selected as counter face to test the new developed ceramic materials.

In all the performed tests, the friction coefficients of the two monolithic silicon nitrides are very similar and slightly lower than the one exhibited by the $Si_3N_4$–TiN composite. As examples, the evolution of the friction coefficients on the three samples, as a function of covered distance, is displayed in Fig. 7a for the test carried under a linear speed of 25 cm $s^{-1}$ and a normal load of 10 N, and in Fig. 7b the data recorded during the tests under the mildest conditions of sliding speed (10 cm $s^{-1}$), load (7 N) and covered distance (790 m). As clearly showed in Fig. 7a, the friction coefficients are quite similar, with values around 0.1, for the two monolithic silicon nitrides sintered with the addition of bioactive glass and MgO. Whereas in the case of the $Si_3N_4$–TiN composite, the coefficient of friction is slightly higher (0.13–0.15) and this value continues to increase slightly increasing the distance.

A possible relationship can be drawn between the friction coefficient and the wetting angles against BS, being the latter around 40° and 50° for $Si_3N_4$–MgO and $Si_3N_4$–bioactive glass, respectively, and around 60° for the composite. When the wetting angles are lower than about 50°, the behaviour of the two parts during sliding is similar, while a lower wettability reduces the lubrication and induces an increase of the friction among the two parts in contact. Only the mildest test conditions (Fig. 7b) put in evidence that, after a distance of 800 m, the three measured friction coefficients are inversely related to the wetting angle (Table 4). In all the other tests, as load and speed increase, the behaviour of the two monolithic silicon nitrides is generally very similar and can be represented by curves similar to those represented in Fig. 7a.

**Table 4** Friction coefficient for the three silicon nitride-based ceramics at different wear test conditions

| Sample | Contact angle (°) | Friction coefficient conditions | | |
|---|---|---|---|---|
| | | 790 m 7 N, 10 cm $s^{-1}$ | 2,200 m 10 N, 25 cm $s^{-1}$ | 12,000 m 10 N, 32 cm $s^{-1}$ |
| $Si_3N_4$–bioactive glass | 50.1 | 0.16 | 0.10 | 0.09 |
| $Si_3N_4$–MgO | 40.3 | 0.13 | 0.10 | 0.09 |
| $Si_3N_4$–TiN | 59.2 | 0.18 | 0.15 | 0.16 |

All the values of the friction coefficient can be considered reasonably low for bearing surfaces in biomedical applications; in fact, they are slightly lower that those concerning other materials commonly used for biomedical devices, e.g. uncoated Co–Cr–Mo alloys previously studied under similar conditions and other alloys coupled to the same polycrystalline alumina in analogous conditions [37].

The designed tribological tests, properly set up under different experimental conditions, clearly indicated the independence of the friction coefficient from load, linear speed and covered distance. This is an important feature, suggesting that, from the point of view of the friction coefficient, these materials coupling could be applied to people with different body weight and activity.

Concerning the surface degradation due wear, only the most severe condition employed, i.e. 10 N, 32 cm $s^{-1}$ and 12,000 m, allowed to observe the wear insurgence on the alumina balls or on the silicon nitride discs. In all the other cases, neither weight loss nor profile relieves were appreciable on both ball and discs, indicating a mutual excellent wear resistance. In fact, it has to be underlined that the track depth on the disk measured after only 790 m of sliding contact of alumina on BioDur® alloys was about 6 μm on the disc [37].

The profiles of the tracks measured at the end of the most severe tribological test repeated four times are reported in Fig. 8 for the $Si_3N_4$–TiN composite. This is the only wear track that was possible to reveal sufficiently by profile relieves. In the reported example, the tracks profiles are quite similar in terms of both depth and width, as also pointed out from the values in Table 5, suggesting a highly homogeneous material and homogeneously prepared sample surface.

As far as the other two samples are concerned, even in the most severe condition wear track on the disk was not clearly detectable, as illustrated in Fig. 9 for the $Si_3N_4$–bioactive glass. Such result indicates that the two monolithic materials have a higher wear resistance toward alumina with respect to the composite $Si_3N_4$–TiN and, also in this case, the effect of the wetting by the liquid medium could be a factor influencing the wear resistance, like in the case of the friction coefficient.

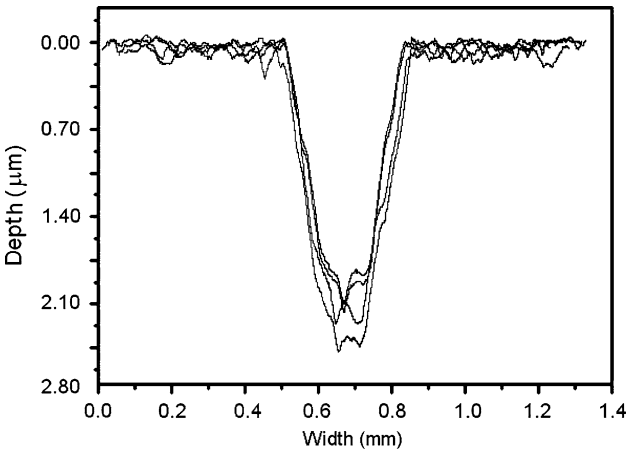


**Fig. 8** Wear tracks profiles registered on the $Si_3N_4$–TiN discs after the tribological test under experimental conditions of 32 cm $s^{-1}$, 10 N (37°C; dilute bovine serum)

Moreover, at this condition, the two monolithic silicon nitride-based ceramics were able to wear the alumina ball, as shown from the measure of the ball width in Table 6.

The microstructural features of the samples after the wear tests are in agreement with the above reported results. The tracks can be hardly revealed only after the long tests at the heaviest adopted conditions. Two examples are reported in Figs. 10a, b and 11a, b, related to the samples $Si_3N_4$–bioactive glass and $Si_3N_4$–TiN, respectively.

**Table 5** Wear tests results for the $Si_3N_4$–TiN composite (12,000 m of covered distance with a normal load of 10 N and a sliding speed of 32 cm $s^{-1}$)

| Test | Depth (μm) | Width (mm) | Area ($mm^2$) | Volume ($mm^3$) | Abrasive wear rate ($mm^3\ N^{-1}\ m^{-1}$) |
|---|---|---|---|---|---|
| 1 | 2.07 | 0.333 | $4.03 \times 10^{-4}$ | $2.28 \times 10^{-2}$ | $2.017 \times 10^{-7}$ |
| 2 | 2.15 | 0.350 | $4.82 \times 10^{-4}$ | $2.73 \times 10^{-2}$ | $2.416 \times 10^{-7}$ |
| 3 | 2.38 | 0.370 | $5.54 \times 10^{-4}$ | $3.13 \times 10^{-2}$ | $2.774 \times 10^{-7}$ |
| 4 | 2.06 | 0.344 | $4.22 \times 10^{-4}$ | $2.38 \times 10^{-2}$ | $2.113 \times 10^{-7}$ |
| Average | 2.16 | 0.349 | $4.65 \times 10^{-4}$ | $2.63 \times 10^{-2}$ | $2.330 \times 10^{-7}$ |

**Table 6** Wear of alumina ball width after the ball-on-disc test with the three silicon nitride based ceramics (original ball diameter: 6 mm; 12,000 m covered; 10 N; sliding speed: 32 cm $s^{-1}$)

| Sample | Wear of alumina ball (Δ mm) |
|---|---|
| $Si_3N_4$–bioactive glass | 0.49 |
| $Si_3N_4$–MgO | 0.28 |
| $Si_3N_4$–TiN | 0.37 |

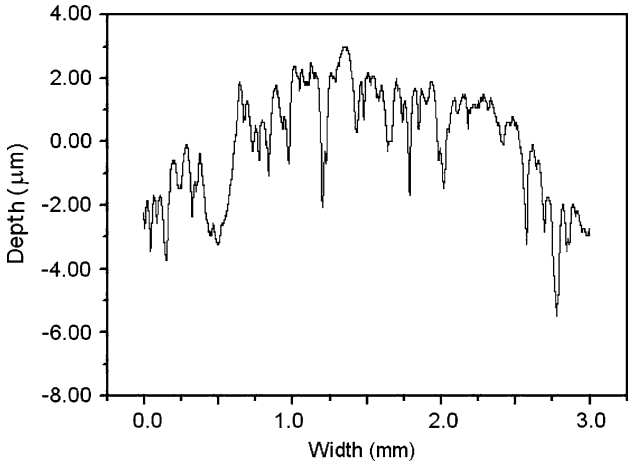


**Fig. 9** Roughness pattern of the $Si_3N_4$–bioactive glass disc area recorded across the track produced after the tribological test (12,000 m covered; 10 N load; of 32 cm $s^{-1}$ sliding speed, 37°C, dilute bovine serum)

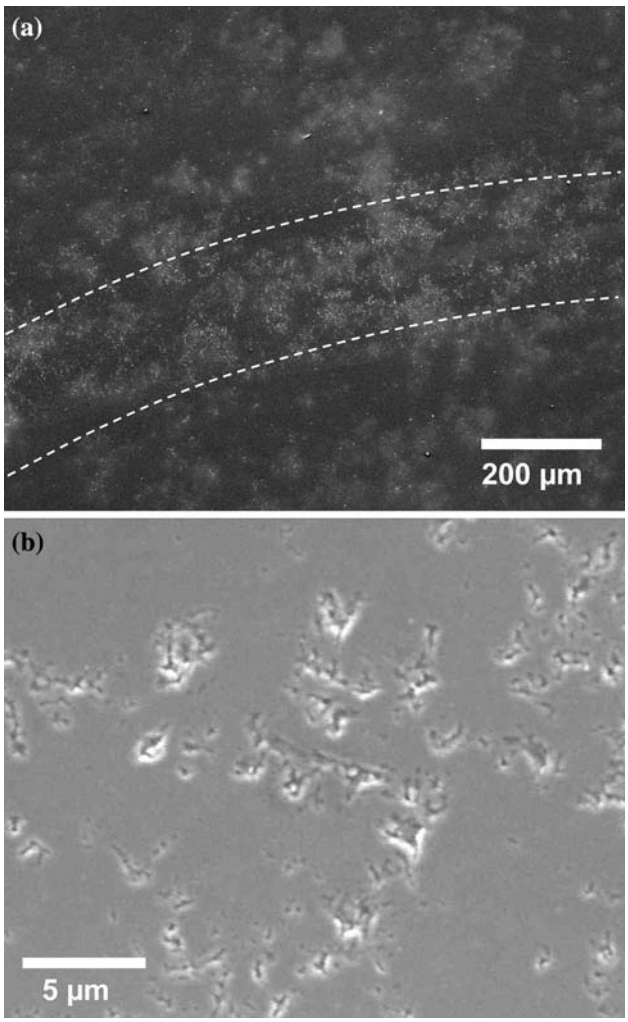


**Fig. 10** (**a**, **b**) track on the surface of the $Si_3N_4$–bioactive glass disc sample produced during the ball-on-disc (∅ 18 mm) wear test (**a**) and relative microscale induced defects (**b**). Test conditions (instr. precision ±0.02): 12,000 m; 10 N, 32 cm $s^{-1}$ in dilute bovine serum

In both the monolithic ceramics the area that underwent the contact with the alumina ball presents some depletion of grain boundary phases and the formation of very small micron-sized defects (Fig. 10b). It is a morphology similar to those observed during chemical etching tests, that induce the leaching of the glassy silicate phases which concentrate at grain boundaries or at triple points. Therefore, the observed surface degradation, although very slight, is probably the consequence of a tribochemical-induced dissolution of the grain boundary phases, that, on the other hands, are also less hard than the silicon nitride phases.

In the $Si_3N_4$–TiN composite, the only where the wear rate was detectable, a preferential removal of grain boundary phases was evidenced too. No pull-out of TiN grains was revealed. However, differently from the previous reported data on the monolithic ceramic, traces of oxygen were found with EDS analyses on the TiN particles. At the same time also an increase of Al was detected either on the $Si_3N_4$ grains or on the TiN particles. Two concurrent phenomena contribute to the wear behaviour: (i) a slight oxidation of TiN, and (ii) a material removal by friction, that leaves a very thin slag of alumina deriving from the contact of the alumina ball with the $Si_3N_4$–TiN surface. Both the factors enhance the friction coefficient as the test duration increase (Fig. 7a).

The difference between the monolithic silicon nitrides and the composite silicon nitride–titanium nitride can derive from the highest hardness of the formers with respect to the latter [1], and from the higher hardness of $Si_3N_4$ in comparison to TiN. Besides, in the monolithics the grain boundary phase removal seems the key feature for the wear performance; no deposit from the alumina ball forms on the worn area. The overall surface degradation is at the limit of the detectability, because the volume of the grain boundary phase is very low (5–10 vol.%). On the contrary, in the composite the presence of a relevant volume (35 vol.%) of TiN particles, softer than silicon nitride, facilitate the surface material removal by abrasion during sliding in contact with the harder alumina ball. At the same time, a very thin

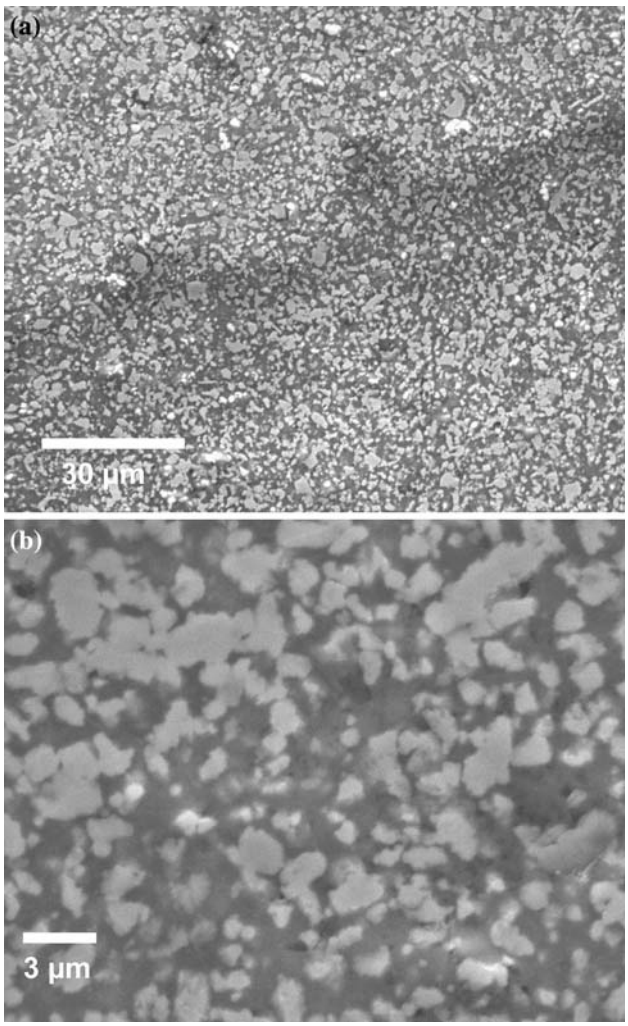


**Fig. 11** (**a**, **b**) Track on the surface of the $Si_3N_4$–TiN disc sample produced during the ball-on-disc (∅ 18 mm) wear test (**a**) and relative microscale induced defects (**b**). Test conditions (instr. precision ±0.02): 12,000 m; 10 N, 32 cm $s^{-1}$ in dilute bovine serum

alumina layer spreads and adheres on the area that comes in contact with the ball. This phenomenon could be facilitated by the lowest wettability of the ceramic surface from the BS and by the consequent highest friction coefficient above reported, compared to the two monolithic ceramics, in conditions simulating the biological environment.

The explanation of the tribological performance of materials and the definition of the mechanisms inducing the phenomena that lead to the observed behaviour during the sliding of the surfaces in contacts are very complex issues, being the interaction between the two mating surfaces depending on the characteristics of the materials and of the surfaces properties, on the experimental conditions and environments. Some works in literature examine the problems related to the wear performance of different couples potentially of interest for joint replacement [3, 15, 38–40]. In those works, results show different conclusions about the wear behaviour of silicon nitride-based materials, although it is rash to make direct comparisons because of the different testing procedures and the different materials, which are not generally described in details. It is in fact well known that composition and microstructure of ceramics deeply influence the properties, including the wear. In silicon nitride, the need to add sintering aids to obtain fully dense bodies, can be regarded as a powerful tool to design ceramics with proper performance for selected applications. In the present study, materials design and controlled processing procedures were adopted to tailor properties for biomedical and wear-resistant applications of silicon nitride. The measured friction coefficients (in the range 0.09–0.18) are lower than those (0.2–0.4) previously reported for tests on silicon nitride against himself in BS solutions or other liquid environments [3, 39, 41], where the high coefficient of friction and specific high wear rates are explained on the basis of strong surface modifications, ascribed to tribochemical reactions [39]. Similar features were not observed on the tests carried out in the present study, the wear rate measured on the composite $Si_3N_4$–TiN is at least one order of magnitude lower that those reported in Ref. [41], moreover, the wear rate was lower than the detectability limit in the monolithic materials. A possible explanation of the different results achieved in the present study, compared to literature data, can lie in the characteristics of the starting materials: in this work, careful attention was devoted to select starting powders and additives and to control the processing procedures, while the materials examined in the literature are "industrial products" not better described.

## 4 Conclusions

Three different silicon nitride-based ceramics (two monolithics and a composite containing TiN) were produced with careful design of the composition of grain boundary phases.

Several properties critical to biomedical applications were examined: wetting behaviour and chemical stability against aqueous media, wear performance under conditions simulating the ones typical of the hip joint prosthesis. The results can be summarized as follows.

*Wettability*: the contact angles of water is significantly lower in the three different silicon nitrides in comparison with those observed on oxide ceramics (alumina and zirconia). In silicon nitride-based materials, contact angles decrease in function of the amount of silicatic grain boundary phases.

The contact angle of Hank's solution PHS2 is similar on the two monolithic silicon nitrides and on alumina, with very low values (around 45°); instead, the contact angles

using BS exhibit a complex behaviour, and the lowest values, again, concern the two monolithic silicon nitrides.

*Chemical stability and corrosion resistance* in water and physiological solutions point out a very low surface modification in the two monolithic silicon nitrides, where the only nearly negligible effects could be associated to the leaching of the grain boundary phases and a possible reaction of silicon nitride to silica. Both these effects are hardly detectable by XPS technique and SEM analyses. The composite $Si_3N_4$–TiN evidences a limited oxidation of TiN to titania $TiO_2$ and a very scarce dissolution of the grain boundary phases.

*Tribological behaviour*: disc (silicon nitride)-on-ball (alumina) wear resistance tests and the measurement of the friction coefficients, carried out at 37°C in dilute BS liquid under conditions simulating those of the human articular hip joint evidence:

(i) very low and constant friction coefficients for the two monolithic ceramics (about 0.1) while in the $Si_3N_4$–TiN composite the coefficient increases to about 0.14. These behaviours were discussed in terms of surface wettability and covered distance.
(ii) Undetectable surface modifications and wear tracks in the monolithic silicon nitrides.
(iii) In the $Si_3N_4$–TiN composite, the only where the wear track was revealed, a preferential removal of grain boundary phases was observed, associated with a slight oxidation of TiN and material removal by friction, maybe due to the lower hardness of TiN in comparison to alumina.

These behaviours are discussed on the basis of the materials physical properties and of the wettability. In any case the friction coefficients are lower than results shown in literature and the wear resistance is one order of magnitude higher than those reported for silicon nitrides.

The silicon nitride-based materials produced and characterized in this work may serve as biomaterials for bone and articular substitutions, also in load bearing prosthesis; in this case the monolithic silicon nitrides are preferred.

## References


1. M. Mazzocchi, A. Bellosi, J. Mater. Sci. Mater. Med. doi: 10.1007/s10856-008-3417-2
2. C.C. Sorrell, P.H. Hardcastle, R.K. Druitt, E.R. Mc Cartney, in *Proceedings 5*th *Meeting and Seminar on: Implants for Spine. Ceramics, Cells and Tissues annual conferences*, Faenza, Italy, ed. by A. Ravaglioli, A. Krajewski (ISTEC-CNR, 1999), p. 47
3. Y.S. Zhou, K. Ikeuchi, M. Ohashi, Wear **210**, 171 (1997)
4. M. Amaral, M.A. Lopez, R.F. Silva, J.D. Santos, Biomaterials **23**, 857 (2002)
5. H.R. Maier, C. Ragoss, M. Held, T. Reske, A. Neumann, K. Jahnke, CFI/Ber. DKG. **81**, 33 (2004)
6. Y.S. Zhou, N. Tomita, K. Ikeuchi, M. Ohashi, K. Takashima, Mater. Sci. Eng. C **5**, 125 (1977)
7. A. Neumann, M. Kramps, C. Ragoss, H.R. Maier, K. Jahnke, Werkstofftech **35**, 569 (2004)
8. A.G. Sulzer, Joint. Endoprostheses. Patent GB1463948, 1977
9. R.L. Diaz, D.D. Ehlert, D.R. Campbell, US Patent 0220679A1, 2004
10. I. Fukuura, S. Niwa, Artificial Articulation. US Patent 4.636.218, 1987
11. K. Olsson, J. Li, L. Urban, Composition comprising silicon nitride as a biomaterial for uses in joint prostheses. EP Patent 1064238, 2003
12. M. Akazawa, K. Kato, Wear **124**, 123 (1988)
13. S. Jahanmir, T.E. Fisher, STLE **31**, 32 (1988)
14. T. Murakami, S. Doi, Key Eng. Mater. **218–220**, 521 (2002)
15. G. Willmann, Adv. Eng. Mater. **3**, 135 (2001)
16. C.S. Giannoulis, T.A. Desai, J. Mater. Sci. Mater. Med. **13**, 75 (2002)
17. C.C. Guedes e Silva, O.Z. Higa, J.C. Bressiani, Mater. Sci. Eng. C **24**, 643 (2004)
18. C.R. Howlett, E. McCartney, W. Ching, Clin. Orthop. **244**, 296 (1989)
19. A. Neumann, T. Reske, M. Held, C. Ragoss, H.R. Maier, K. Jahnke, J. Mater. Sci. Mater. Med. **15**, 1135 (2004)
20. R. Kue, A. Sohorabi, D. Nagle, C.G. Frondoza, D. Hungeford, Biomaterials **20**, 1195 (1999)
21. A. Sohrabi, C. Holland, D. Nagle, D.S. Hungerford, C.G. Frondoza, J. Biomed. Mater. Res. **50**, 49 (2000)
22. G. Heimke, G. Willmann, in *Biomaterials Engineering and Devices. Human applications. Vol. 2 Orthopaedic, dental and bone graft applications*, ed. by D.L. Wise et al. (Humana Press Inc., Totowa, NJ, 2000), p. 253
23. A. Bellosi, in *Design and Processing of Non-oxide Ceramic*, ed. by Y.G. Gogotsi, R.A. Andriewski. Materials Science of Nitrides, Borides, Carbides. NATO-ARW Series (Kluwer Academic Publisher, Doordtecht, The Netherlands, 1999), p. 285
24. A. Bellosi, S. Guicciardi, A. Tampieri, J. Eur. Ceram. Soc. 983 (1992)
25. C.C. Annarelli, J. Fornazero, R. Cohen, J. Bert, J.-L. Besse, J. Colloid Interface Sci. **213**, 386 (1999)
26. S. Agathopoulos, P. Nikolopoulos, J. Biomed. Mater. Res. **29**, 421 (1995)
27. M. Amaral, M.A. Lopes, J.D. Santos, R.F. Silva, Biomaterials **23**, 4123 (2002)
28. M. Lampin, R. Warocquier-Clerout, C. Legris, M. Degrange, M.F. Sigot-Luizard, J. Biomed. Res. **36**, 99 (1997)
29. S. Agathopoulos, P. Nikolopoulos, in: *Euroceramics IV*, ed. by A. Ravaglioli. Proceedings of the Fourth Euroceramics, Conference, vol. 8 (Faenza, Italy, 1995), p. 319
30. N. Nicoli Aldini, M. Fini, G. Giavaresi, P. Torricelli, L. Martini, R. Giardino, A. Krajewski, A. Ravaglioli, M. Mazzocchi, B. Dubini, M.G. Ponzi Bossi, F. Rustichelli, V. Stanic, J. Biomed. Mater. Res. **61**, 282 (2002)
31. Å. Rosengren, S. Oscarsson, M. Mazzocchi, A. Krajewski, A. Ravaglioli, Biomaterials **24**, 147 (2003)
32. M.A. Lopez, F.J. Monteiro, A.P. Serro, B. Saramago, I.R. Gibson, J. Biomed. Mater. Res. **45**, 370 (1999)
33. C. Galassi, F. Bertoni, S. Ardizzone, C.L. Bianchi, J. Mater. Res. **15**, 155 (2000)
34. A. Krajewski, A. Piancastelli, A. Malavolti, Biomaterials **19**, 637 (1998)
35. A. Bondanini, F. Monteverde, A. Bellosi, J. Mater. Sci. **36**, 4851 (2001)

36. C.A. Haynes, W. Norde, Colloid Surf. B: Biointerfaces **2**, 517 (1994)
37. S. Spriano, E. Vernè, M.G. Faga, S. Buglioli, G. Maina, Wear **259**, 919 (2005)
38. G. Willmann, CFI/Ber. DKG. **79**(5), 27 (2002)
39. J. Kusaka, K. Takashima, D. Yamane, K. Ikeuchi, Wear **225**, 734 (1999)
40. C.S. Abreau, M. Amaral, F.J. Oliveira, J.D. Santos, R.F. Silva, J.R. Gomes, Key Eng. Mater. **230–232**, 919 (2002)
41. K. Ikeuchi, J. Kusaka, H. Yoshida, J. Ceram. Proc. Res. **1**, 53 (2000)